



HASPIDE-SPACE for solar, magnetar and gamma-ray burst monitoring

**C. Grimani*, L. Servoli, M. Menichelli, M. Villani, M. Fabi, F. Sabbatini, M. Messerotti
and the HASPIDE Collaboration**

***University of Urbino Carlo Bo and INFN Florence, Italy**



HASPIDE-SPACE scientific objectives

- **Space Weather impact on space missions.** To study the spacecraft deep charging (LISA Pathfinder, LISA and Metis/Solar Orbiter) precise and accurate SEP flux observations from tens of MeV up to GeV energies are needed
- **Solar energetic proton flux monitoring** (from MeV through at least 400 MeV)
- **Solar flare detection and short-term forecast:** photon and electron detection in the keV-MeV range, respectively
- **Detection of extragalactic gamma-ray bursts and magnetar flaring**

HASPIDE-SPACE expected performance

- We aim at studying the characteristics of a detector based on **a:Si-H** for long-term monitoring of **medium-intense solar proton energy spectra** ($>10^7$ protons cm^{-2} > 30 MeV) with an uncertainty smaller than 30% up to 400 MeV
- This detector should also allow for X-ray and (hopefully) solar electron observations

Hydrogenated amorphous silicon (a-Si:H) characteristics

- Excellent radiation hardness (same behaviour after TID of 100 Mrad, while after 10^{16} neq(1 MeV) /cm² detector response still linear, with less than 33% modification of sensitivity)
- Amorphous silicon has an intrinsic disordered nature. The number of dangling bonds inside the material must be reduced by introducing H (>1% atomic) into the material to passivate these dangling bonds in order to reduce the leakage current
- It finds application in harsh radiation environments for medical purposes, for particle beam characterization and now also for space instruments
- Mechanically flexible, very thin and light-weighted, low-to-zero power consumption

M. Menichelli, L. Servoli & N. Wyrsh, *Front. Phys.*, 10:943306, 2022



**SEE talk by L. Servoli
tomorrow 10:10**

Solar activity and overall particle flux

ICMEs and HSS

Recurrent and non-recurrent Forbush Decreases

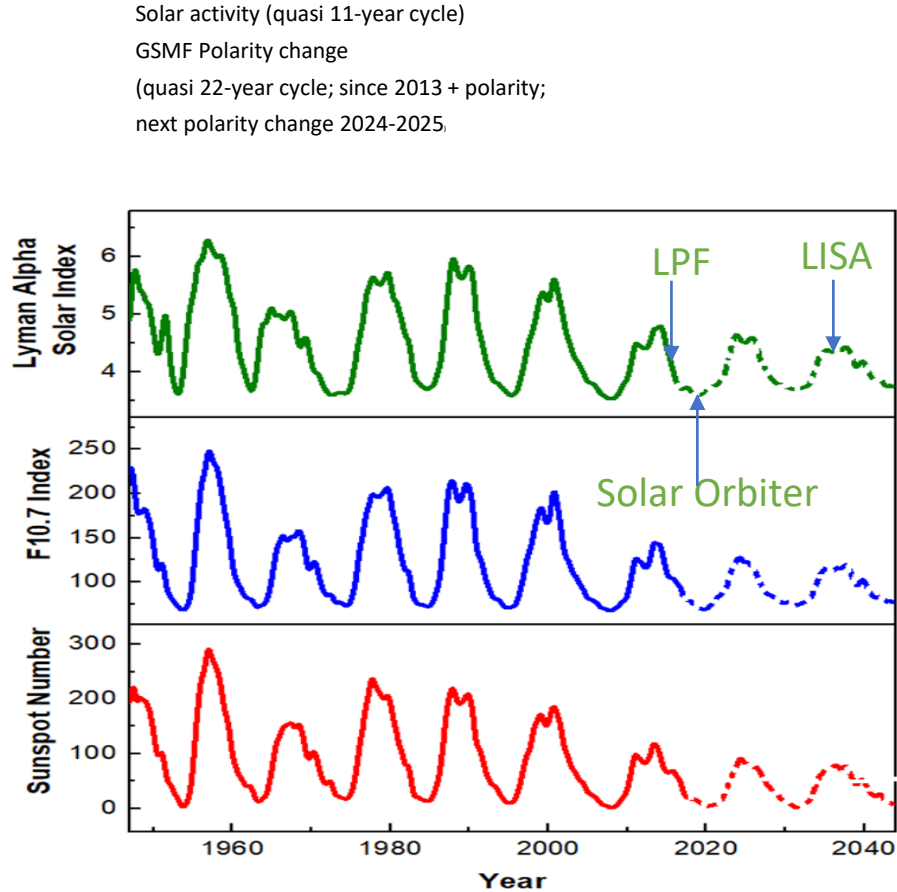
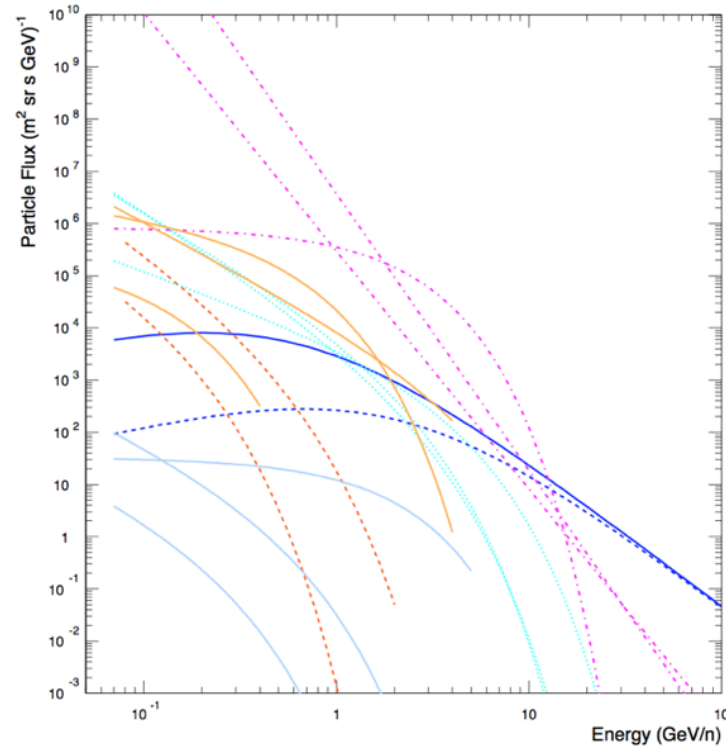


Fig. 5 Monthly variations of the observed and predicted (dotted) values of the sunspot numbers, F10.7 cm index and Lyman alpha index

Singh & Bhargawa Astrophys. Space Sci., 364, 12, 2019

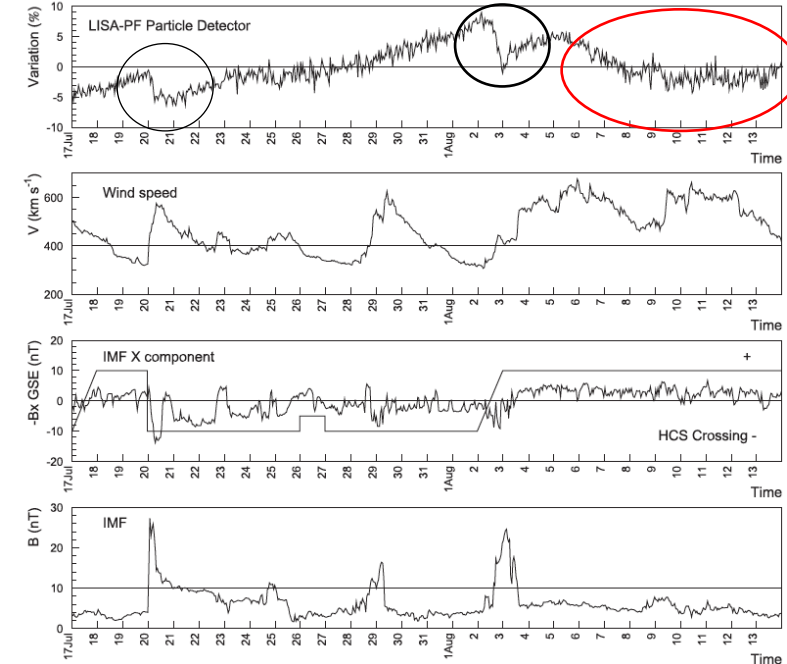


Galactic cosmic-ray protons

SEP February 23, 1956 (p)

SEP December 13, 2006 (p) SEP December 13, 2006 (He)/ 10^4

SEP December 14, 2006 (p)



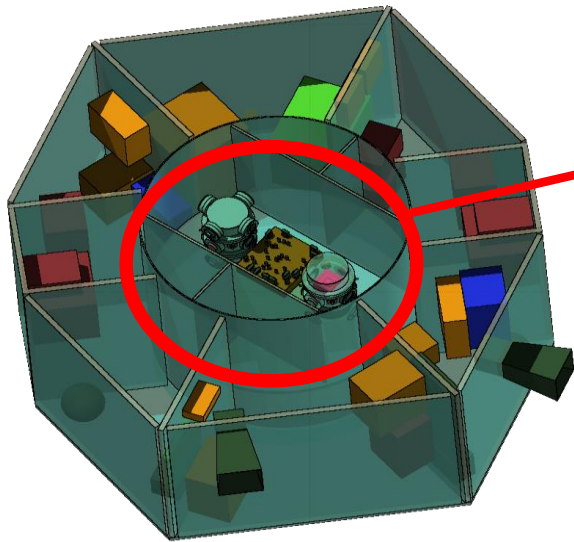
Armano et al.; ApJ, 874, 167, 2019



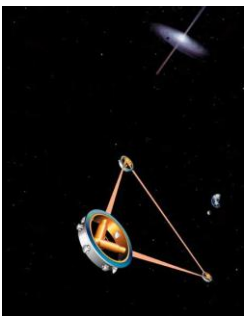
1906
UNIVERSITÀ
DEGLI STUDI
DI URBINO
CARLO BO



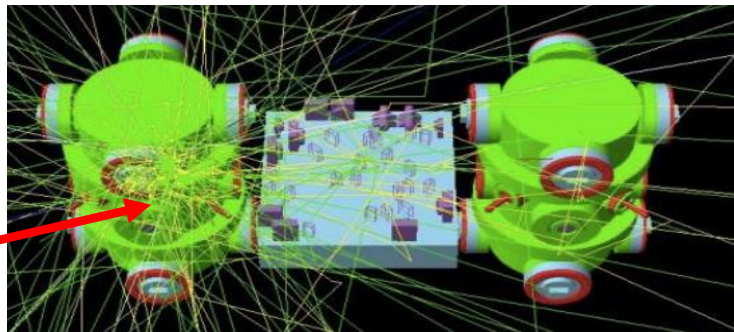
Spacecraft deep charging



LISA PATHFINDER TEST-MASS CHARGING
13.8 g cm⁻² shielding material: protons and nuclei are stopped below 100 MeV(/n)

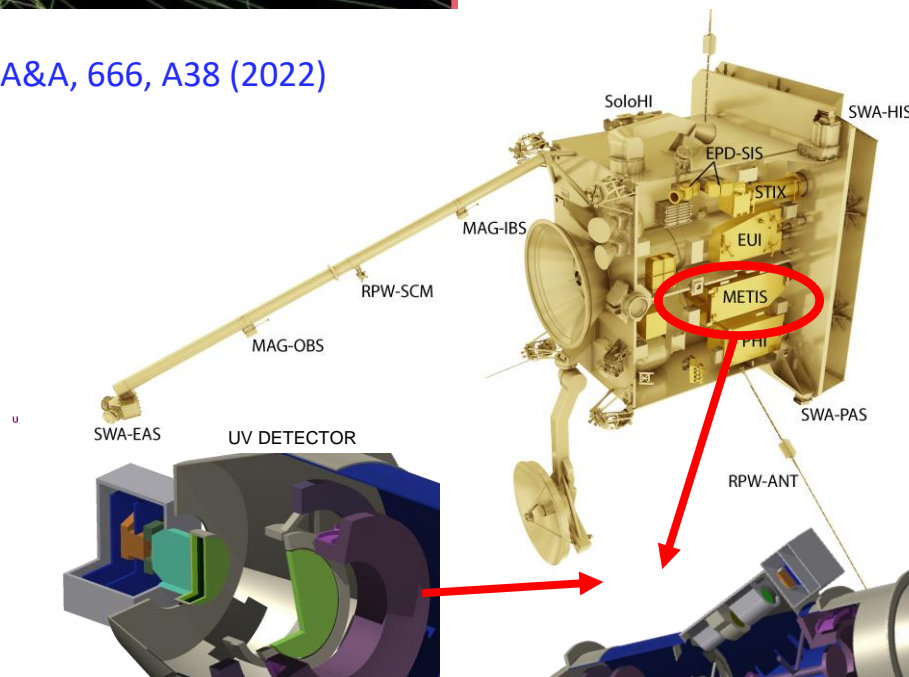


Launch: 2035
Arm: 2.5 10⁶ km
Orbit: Heliocentric -
3 S/C trailing Earth
at 50 million km

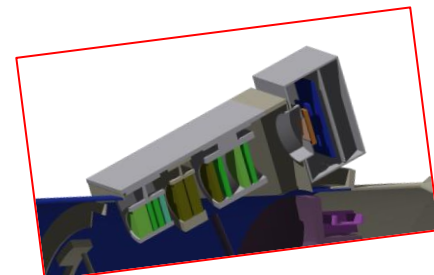


C. Grimaldi et al., A&A, 666, A38 (2022)

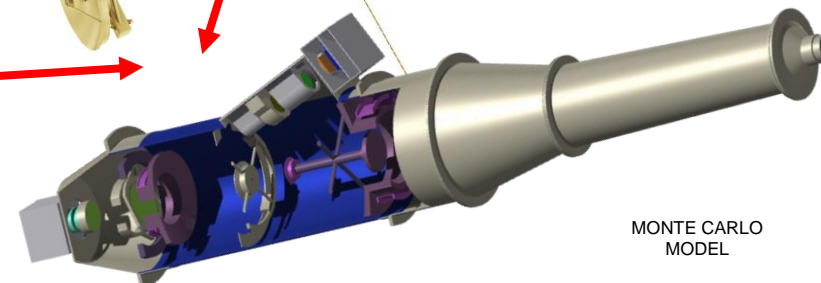
Metis/Solar Orbiter:
>1.2 g cm⁻² shielding material: protons and nuclei are stopped below 40 MeV(/n)



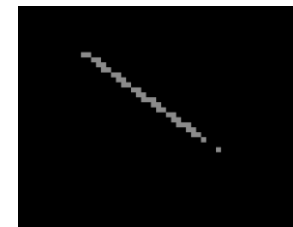
Courtesy of Michele Fabi



VL DETECTOR
Minimum 1.2 g cm⁻² of shielding material



MONTE CARLO
MODEL



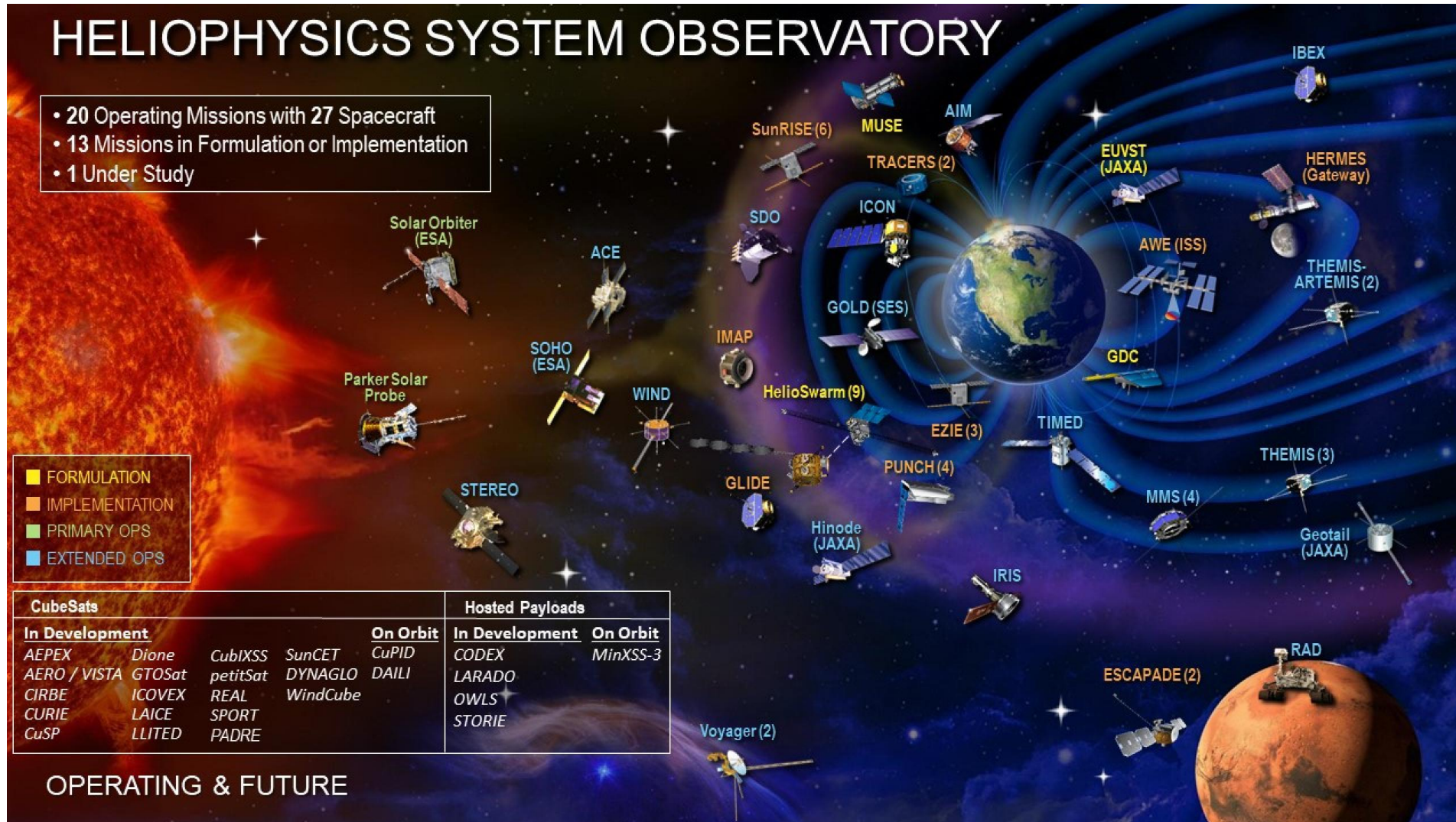
C. Grimaldi et al., A&A, 656, A15 (2021)



1506
UNIVERSITÀ
DEGLI STUDI
DI URBINO
CARLO BO



SEP flux measurements above 100 MeV



- **BepiColombo/BERM** protons up to about 200 MeV
- **HEPD/CSES-01** protons up to 250 MeV (near Earth)
- **SEISS/GOES** protons up to 500 MeV (near Earth)
- **SOHO/EPHIN** protons up to 700 MeV (L1)
- **Solar Orbiter/HET** protons up to 1 GeV? (within 1 au no on soar)
- **AMS-02** on board the Space Station protons > 450 MeV/n (near Earth)



1906
UNIVERSITÀ
DEGLI STUDI
DI URBINO
CARLO BO



X-ray emission from the flare October 28, 2021

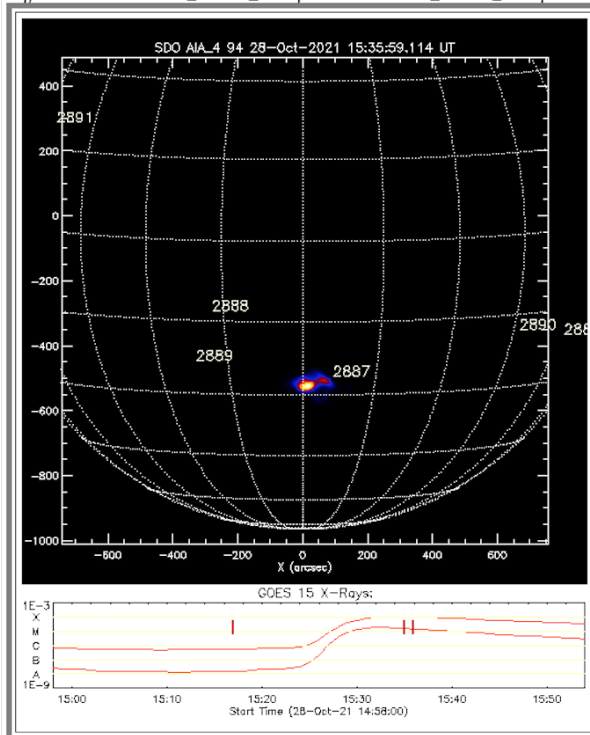
SolarSoft



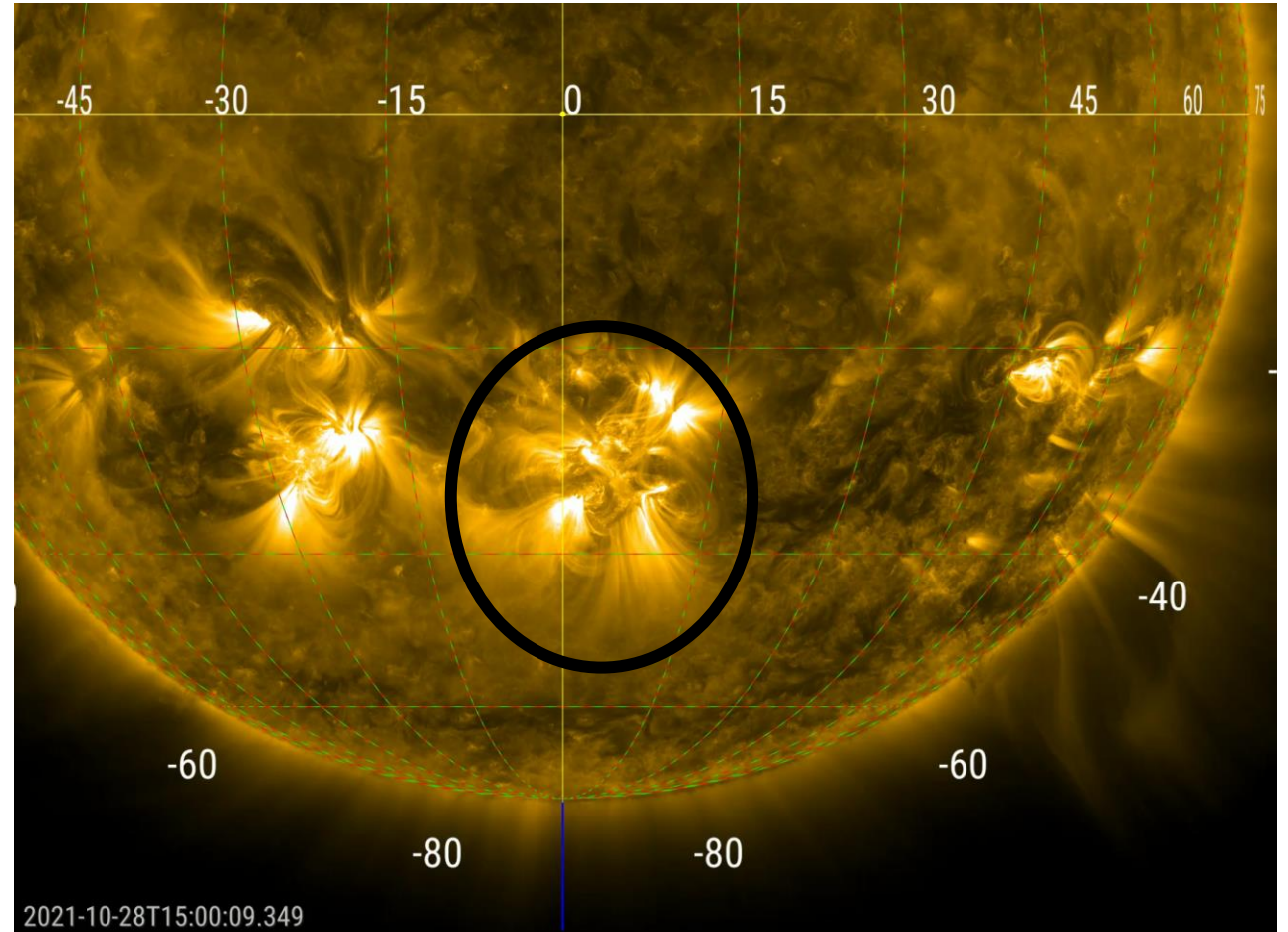
Event#	EName	Start	Stop	Peak	GOES Class	Derived Position
2	gev_20211028_1517	2021/10/28 15:17:00	15:48:00	15:35:00	X1.0	S28W01 (2887)

Flare Locator Image

Difference: AIA20211028_153600_0094.fits - AIA20211028_151700_0094.fits



freeland@lmsol.com



1506
UNIVERSITÀ
DEGLI STUDI
DI URBINO
CARLO BO



October 28, 2021 event: multispacecraft observations

Papaioannu et al., A&A, 660, L5, 9pp (2021)

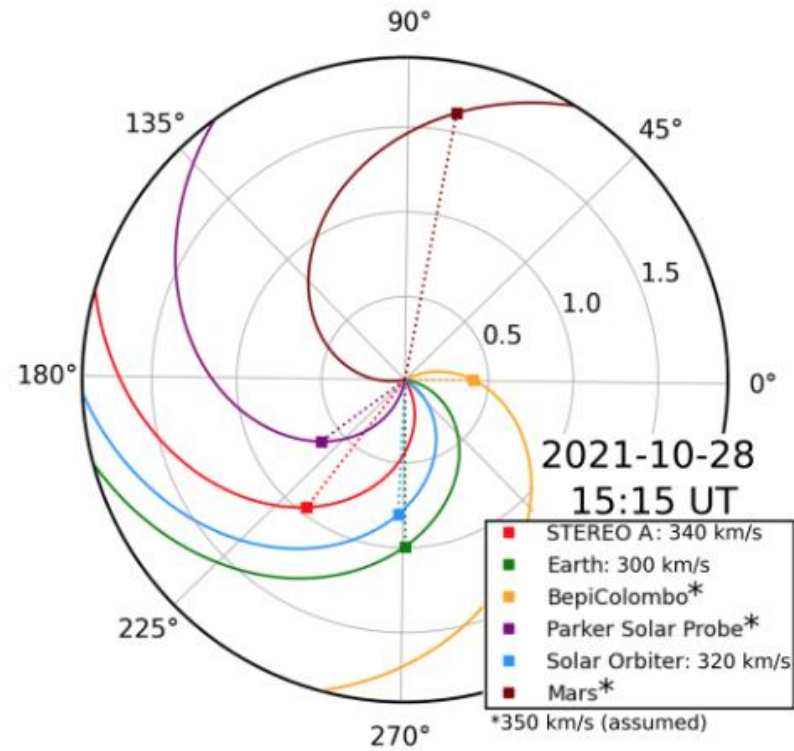


Fig. A.1. A view of the ecliptic plane from solar north showing the positions of various spacecraft on 28 October 2021 at 15:15 UT. The Parker spirals are shown for each spacecraft. From the Solar MAGnetic Connection Haus tool (<https://solar-mach.github.io/>).

X-ray, electron and proton emission October 28, 2021 event

Klein et al., A&A 663, A173, 2022

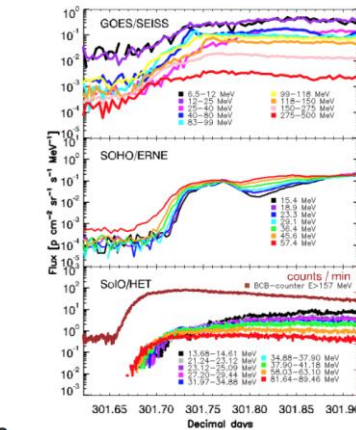
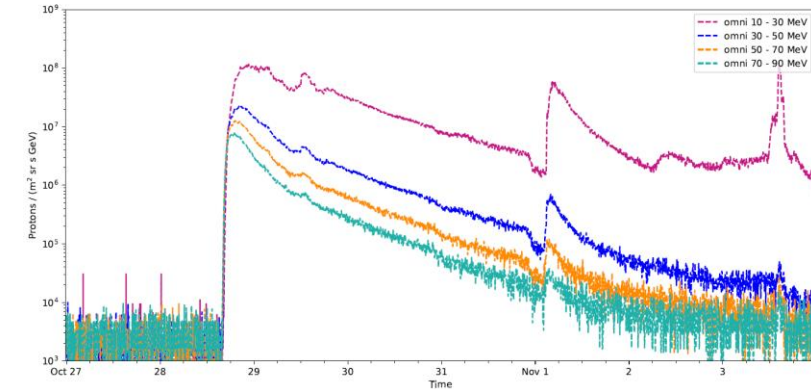
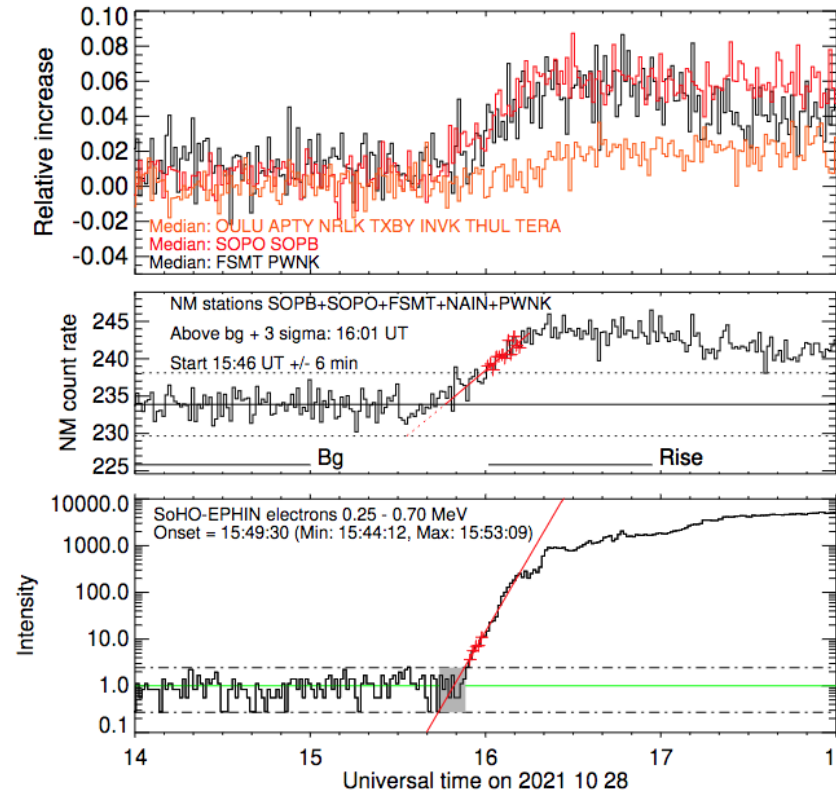
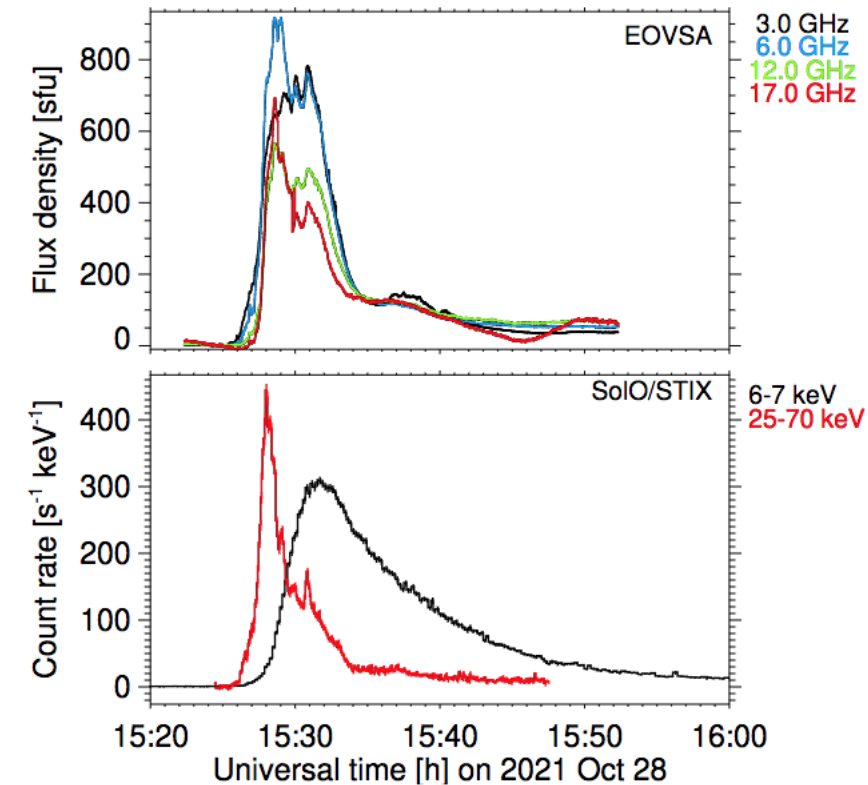
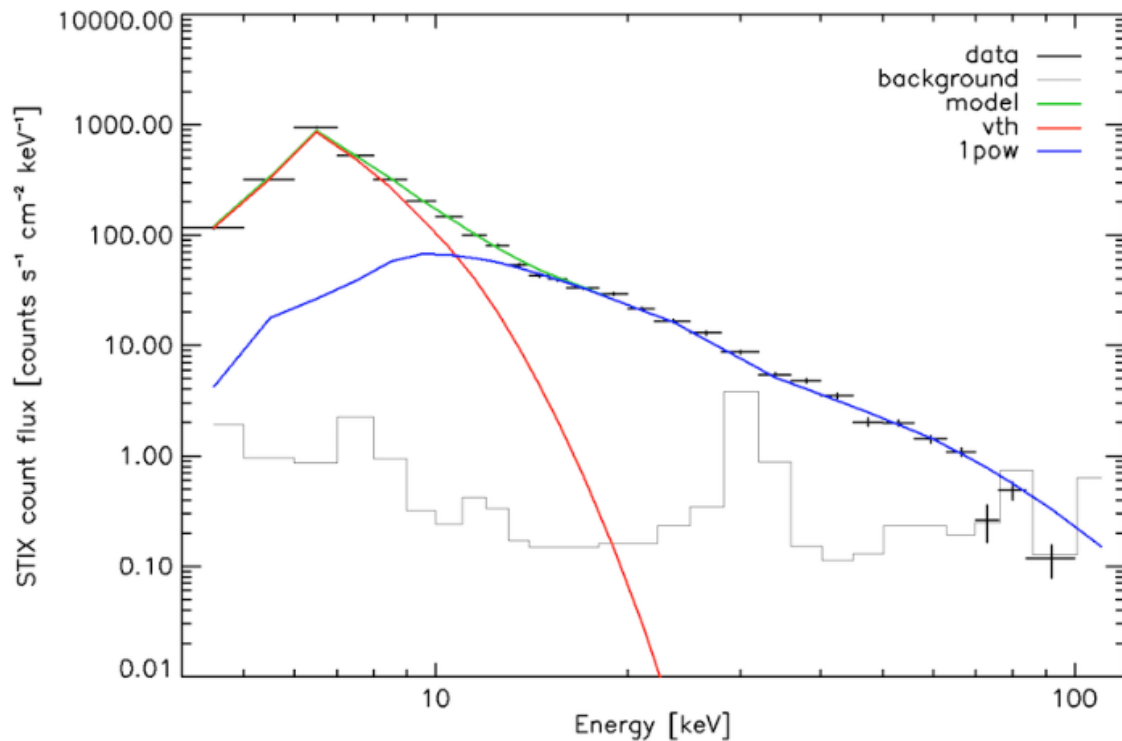


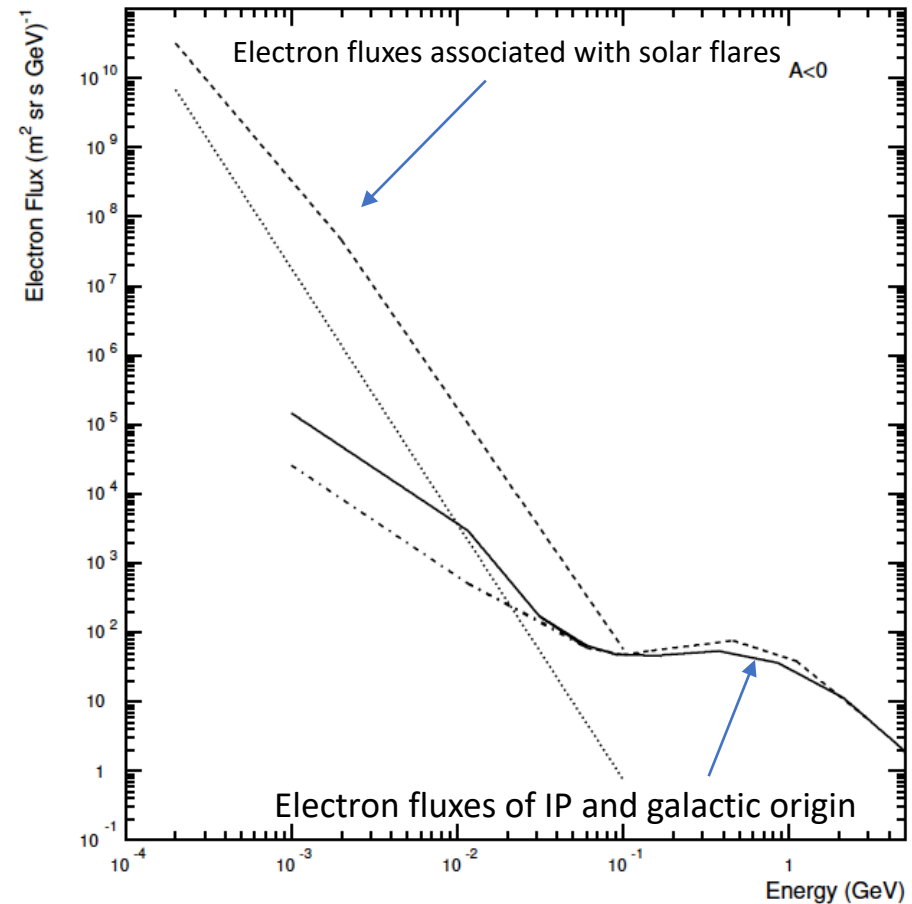
Fig. A.2. Energetic particle recordings of GLE73 in the near Earth space, (from top to bottom) 5-min averaged GOES/SEISS differential fluxes; SOHO/ERNE fluxes and SoI/O/HET measurements including the recordings of the SoI/O/HET/BCB-counter.

Onset after 16.00 UT
Peak NM: 18:00
Peak Space:
20:35-22:35 UT

Photon and electron fluxes from solar flaring



Klein et al., A&A 663, A173, 2022



C. Grimani et al., CQG, 26, 26,15004, 2009



1506
UNIVERSITÀ
DEGLI STUDI
DI URBINO
CARLO BO



October 28, 2021 SEP event: space and NM observations

C. Grimaldi et al., arXiv: 2302.00339,
C. Grimaldi et al., submitted to Astroph. Sp. Sc.
C. Grimaldi et al.; submitted to A&A

Papaioannu et al., A&A, 660, L5, 9pp (2021)

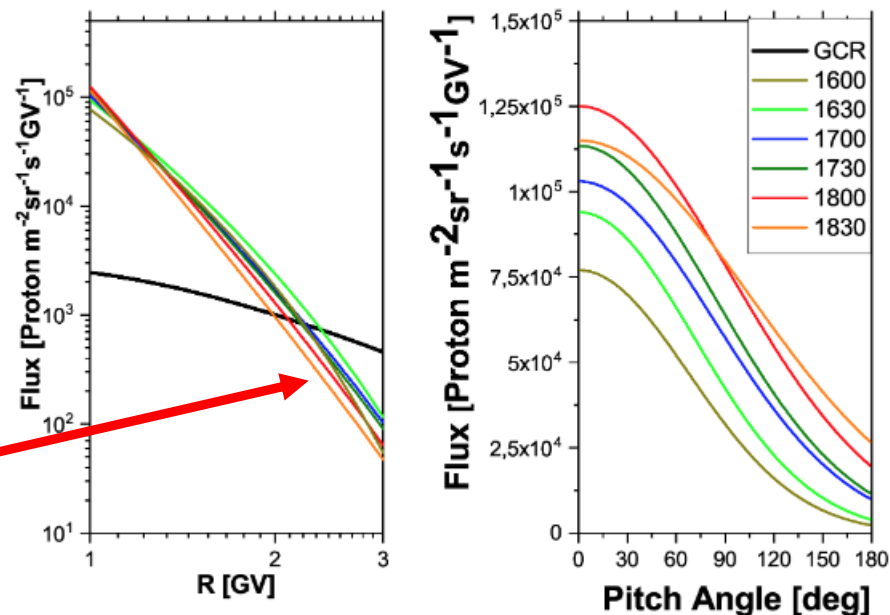
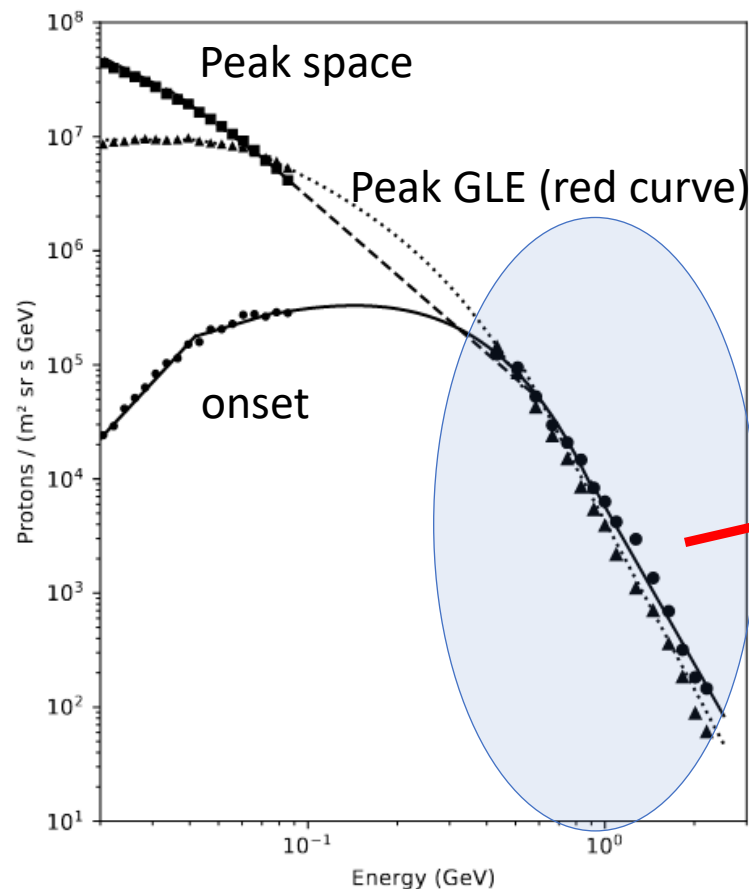


Fig. 4. Derived SEP rigidity spectra (left panel) and PADs (right panel) during GLE73 on 28 October 2021. The solid black line denotes the galactic cosmic ray flux, which corresponds to the time period of the GLE 73 occurrence (see text for details). All time in the legend are in UT and refer to the start of the corresponding five minute interval over which the data are integrated.



1506
UNIVERSITÀ
DEGLI STUDI
DI URBINO
CARLO BO



October 28, 2021 SEP event

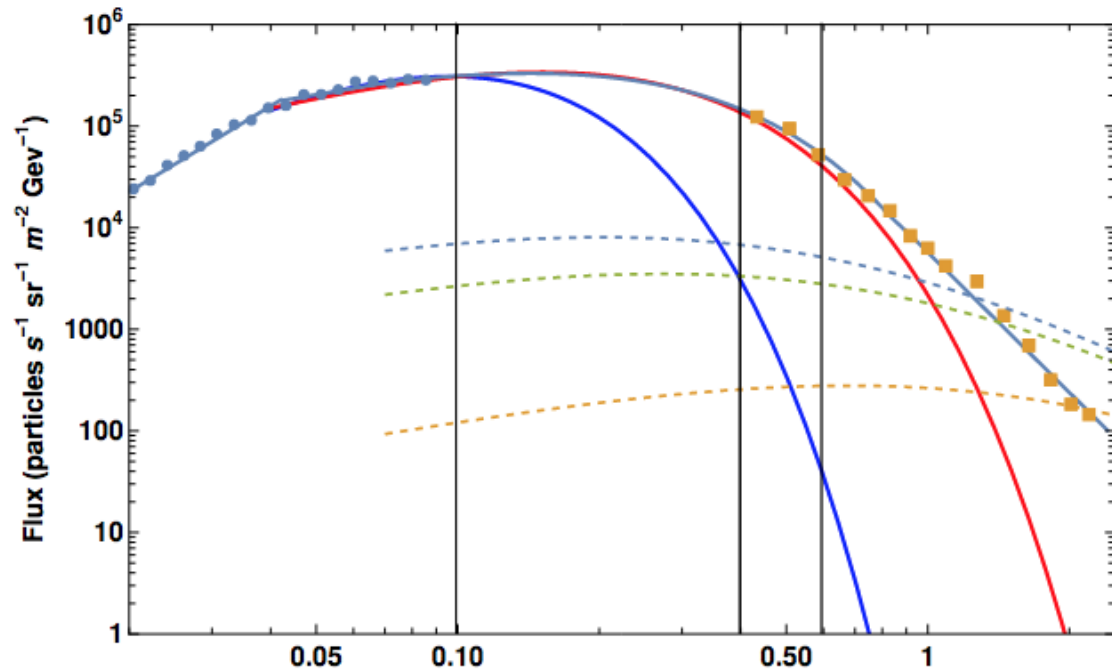
Small/large blue dots: data gathered in space up to 100 MeV with Solar Orbiter/HET.

Orange squares: neutron monitor data.

The blue curve represents the best fit to data up to 100 MeV.

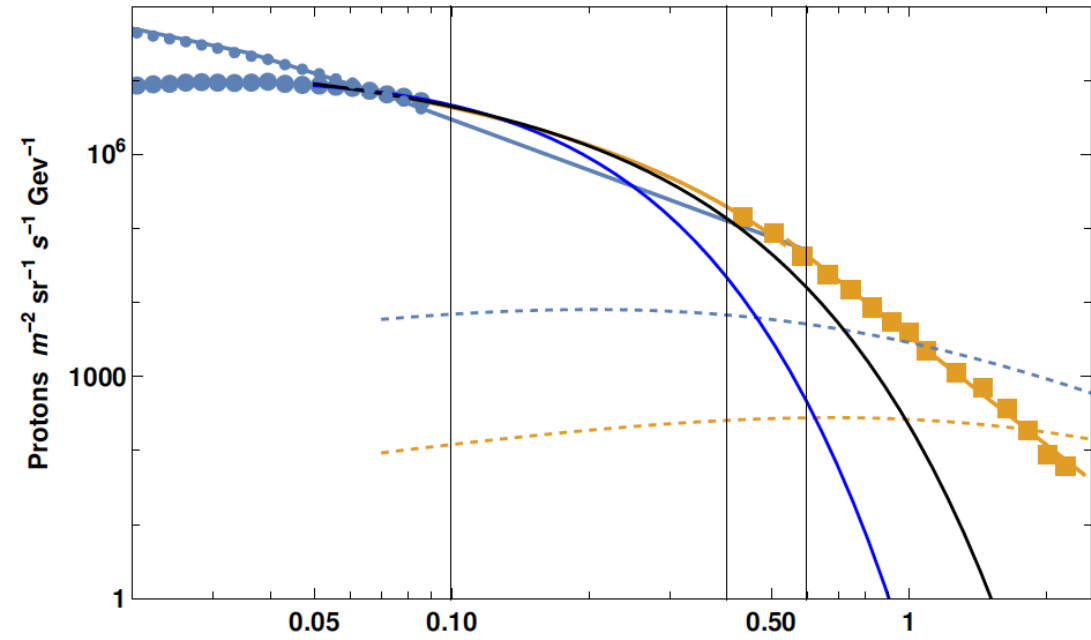
The red curve represents the best fit to data up to 400 MeV \rightarrow SEP monitoring in space should be monitored up to minimum energies of 400 MeV.

Dashed lines: GCR protons.



Event onset

Energy (GeV)

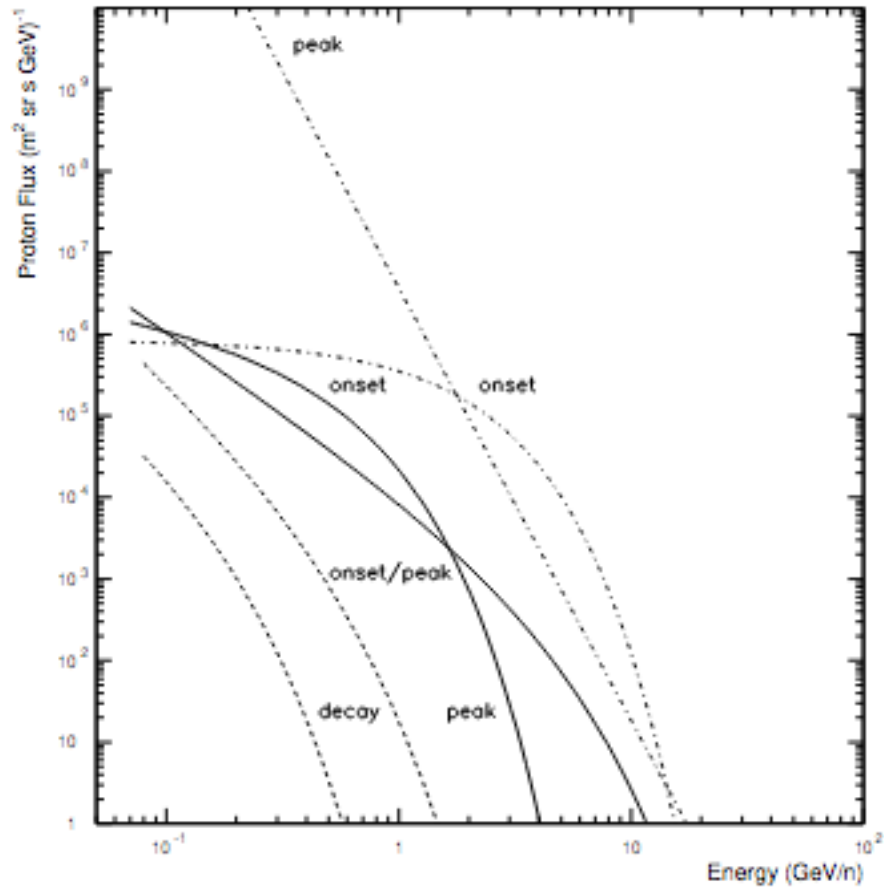


Event peak

Energy (GeV)

C. Grimani et al., arXiv: 2302.00339, submitted to Astroph. Sp. Sc.

GCR and SEP energy distribution



C. Grimani et al.; submitted to A&A

	Solar minimum	Solar maximum	Onset	Peak/Decay
GCR	19%	6%		
SEP 13/12/2006			90%	98% (peak)
SEP 14/12/2006			99%	100% (decay)
SEP 23/2/1956			25%	99.5% (peak)

Proton percentage below 400 MeV



1906
UNIVERSITÀ
DEGLI STUDI
DI URBINO
CARLO BO



Magnetars

- The majority of known magnetars lie within 10 kpc
- Surface magnetic fields: 10^{13} - 10^{15} G
- Periods: 1–10 s
- Birthrate: $\sim 1.5\text{--}3 \times 10^{-3} \text{ yr}^{-1}$ for the
- Progenitor masses: 20-45 solar masses
- Mass: 1.4-1.6 solar masses

Olausen & Kaspi, 2014

- 30 magnetars listed in the **McGill Online Magnetar Catalog** (<https://www.physics.mcgill.ca/~pulsar/magnetar/main.html>)
7 to be confirmed (6+ PSR J1846–0258)
- SGRs and AXPs are believed to be magnetars
- 12 SGRs + 4 candidates
- 12 AXPs + 2 candidates
- Pulsars and magnetars have blackbody temperatures that lie in the X-ray band: a continuous emission arrives from these stars
In addition flaring from these compact objects is observed



Hard X rays and soft gamma rays associated with GRBs and galactic magnetar flaring increase the ionization of ionosphere thus disturbing VLF radio wave propagation in the range of frequencies 3-30 kHz and causing the ozone layer depletion

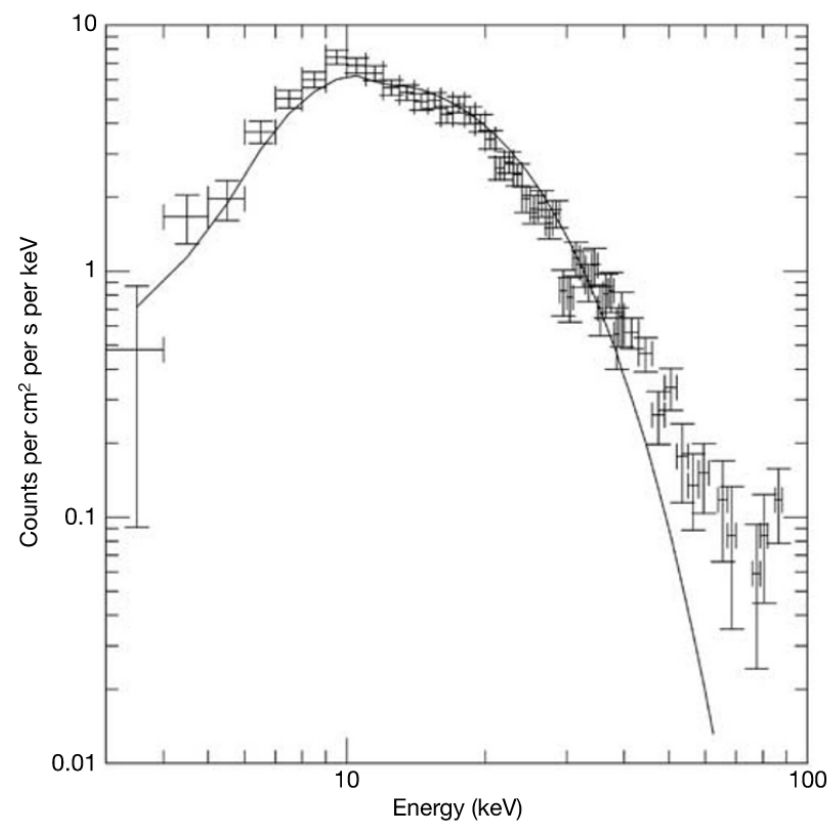
Soviet probes Venera 11, Venera 12 and the German-American solar satellite Helios II were all hit by "off the scale" gamma rays leading to the discovery of soft gamma-ray repeaters

SGR flaring

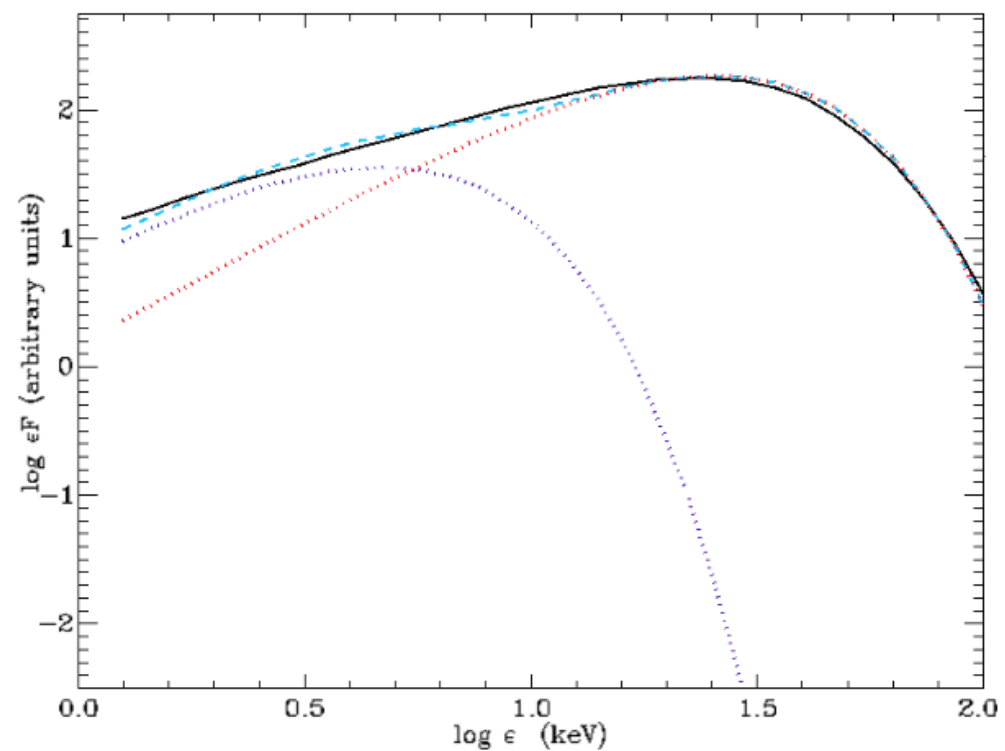
- **SGR 1900+14** : August 27, 1998 at 12.5 kpc from Earth, total hard X-ray and soft gamma emission of 2×10^{44} erg.
- **SGR 1806-20** at 15 kpc from Earth was observed on December 27, 2004.
- Up to 10^{47} erg are expected. The duration is: peak emission < 1 s; tail up to hundreds- one thousand seconds. Afterglow hours for extragalactic GRBs. In general magnetar emit 10^{39} - 10^{42} erg s^{-1} even though the emission may reach 10^{44} erg s^{-1} . Continuous X-ray emission characterized by a few second periodicities and a luminosity of 10^{35} - 10^{36} erg s^{-1} in the range 1-200 keV.
- **Energy most likely beamed.**

SGR 1806-20

SGR 1806-20



Hurley et al., Nature , vol. 434 , 28 April 2005



Taverna & Turolla, Galaxies, 6, 35, 2018

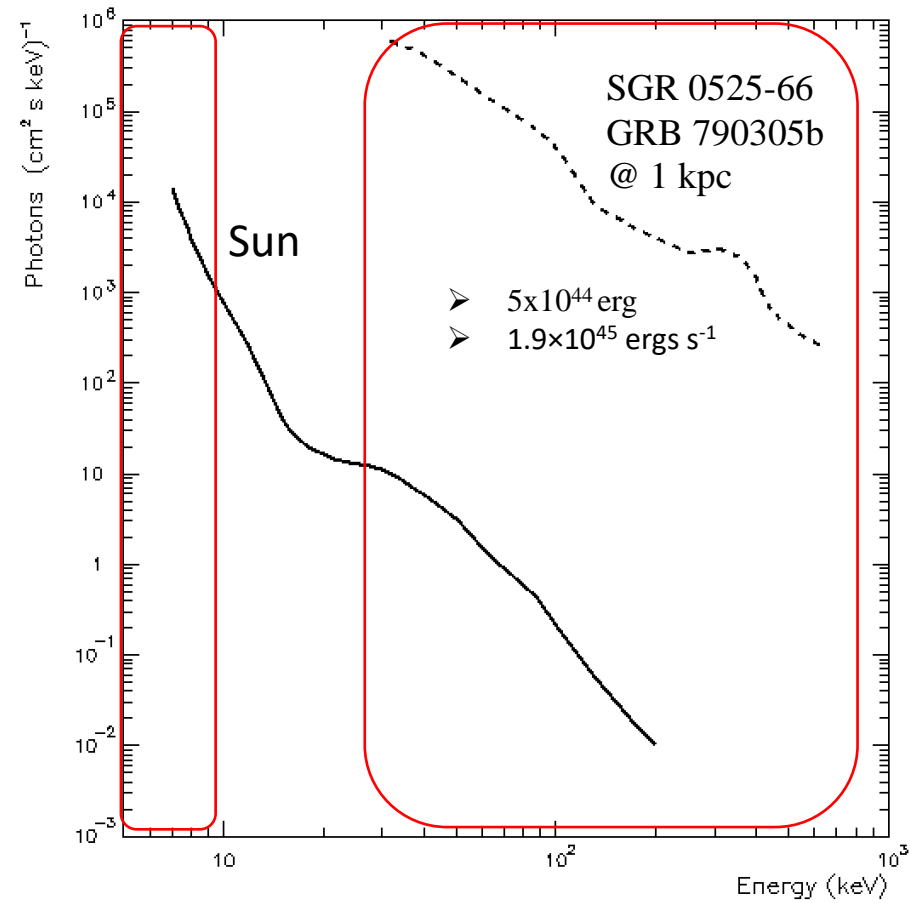


1506
UNIVERSITÀ
DEGLI STUDI
DI URBINO
CARLO BO



Photon fluxes from star flaring

Fenimore, Klebesadel and Laros, ApJ, 460, 964, 1996



Benz et. Liv. Rev. in Sol. Phys., 14, 2, 2017

The brightest gamma-ray burst

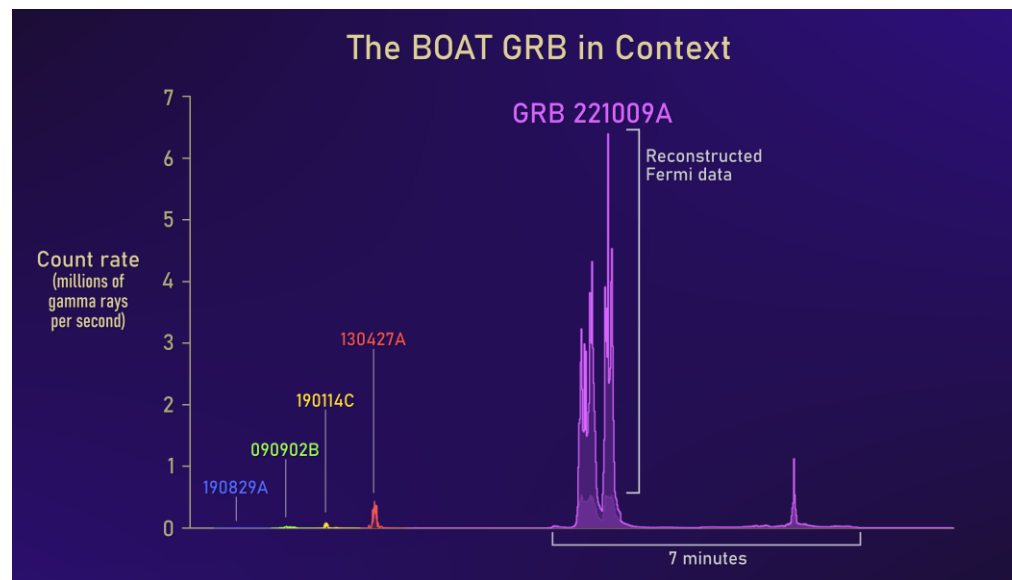
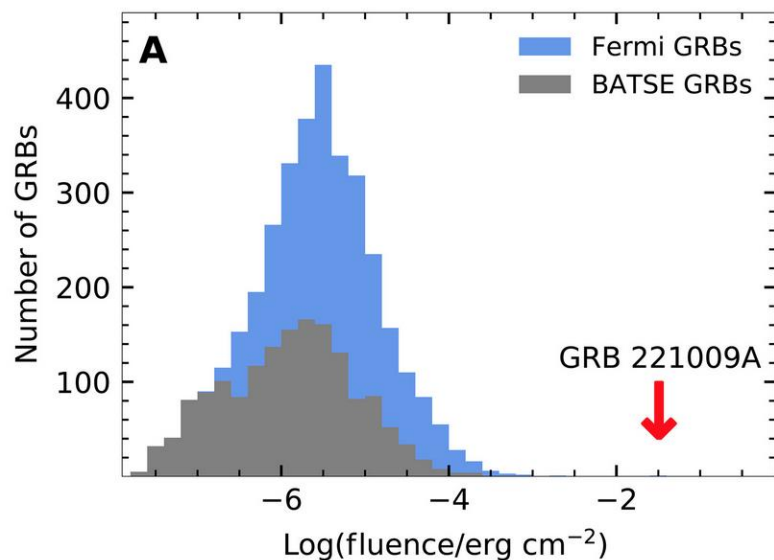
Date: October 9, 2022

Distance: 720 Mpc

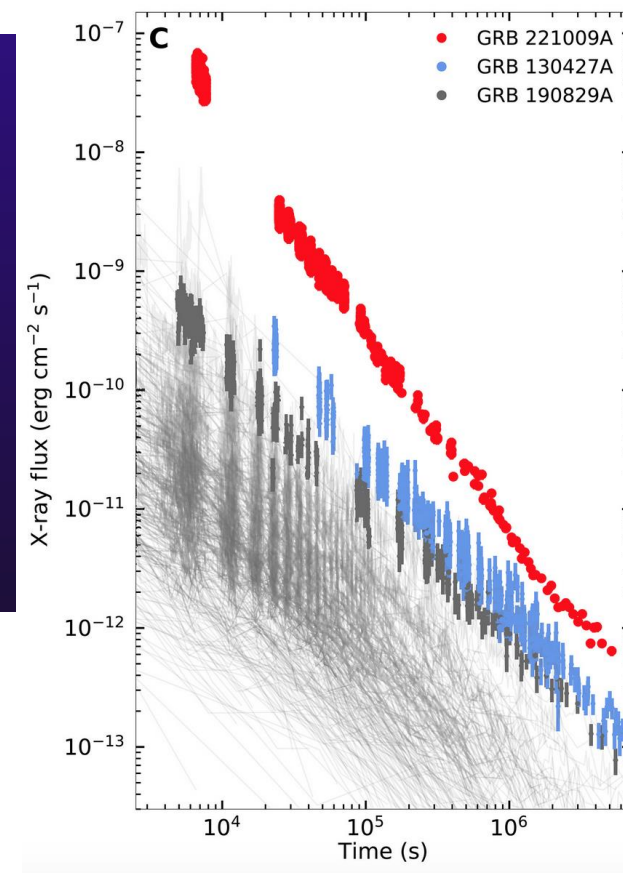
Total energy: 10^{55} erg

Frequency: 1000-10000 years

Maximum photon energy: 18 TeV



Credit: NASA's Goddard Space Flight Center and Adam Goldstein (USRA)



1506
UNIVERSITÀ
DEGLI STUDI
DI URBINO
CARLO BO



Space Weather impact of magnetar flaring

- Disturbance of amplitude and phase of VLF radio wave propagation (3-30 kHz) down to 60 km altitude
- The disturbance appears in coincidence with the RHESSI observations (onset 20 ms and maximum disturbance after 200 ms exponential recovery in less than 500 ms)
- TEC variations (small flare changes TEC by 0.04 TECU)
- Ozone depletion and NO_y density variations:
Photons dissociate N₂ molecules catalyzing the reaction:
$$\text{NO} + \text{O}_3 \rightarrow \text{NO}_2 + \text{O}_2$$
$$\text{NO}_2 + \text{O} \rightarrow \text{NO} + \text{O}_2$$
$$\text{net: } \text{O}_3 + \text{O} \rightarrow \text{O}_2 + \text{O}_2$$

if NO_y density increases, the solar fluence increases ($\geq 10^7 \text{ erg cm}^{-2}$ would destroy the ozone layer)
- DNA damage caused by ozone depletion

Optimization of a a:Si-H detector

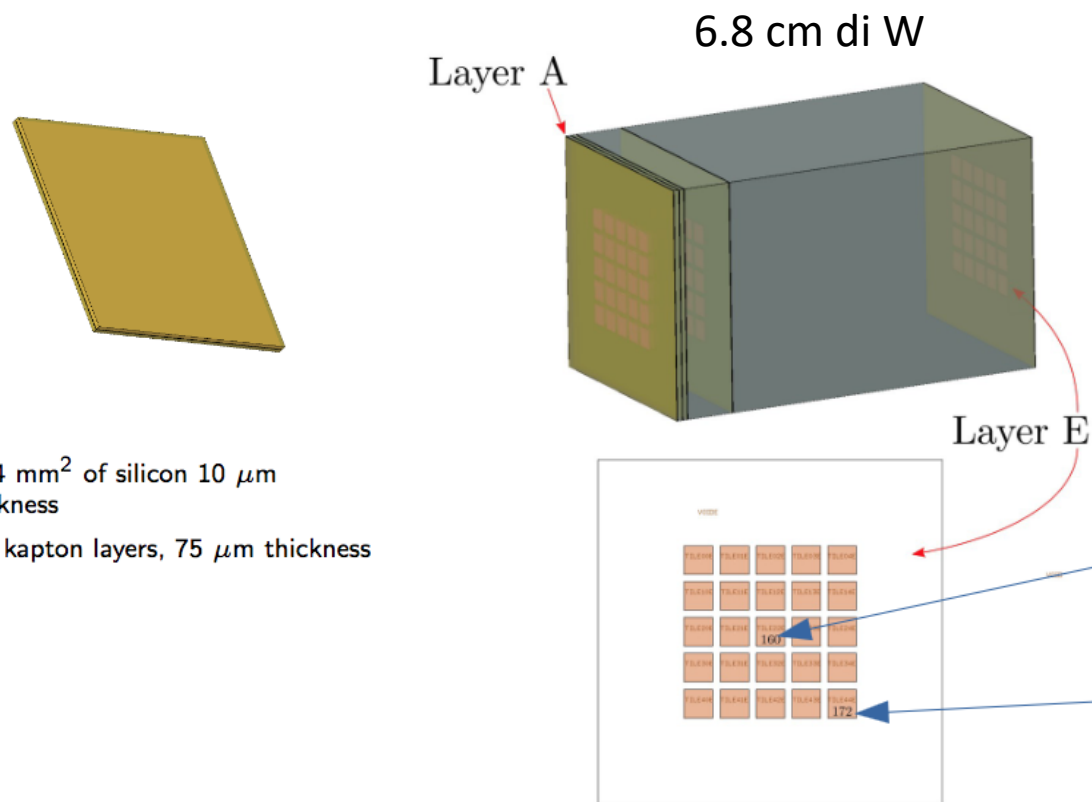
- **a:Si-H active material** and tungsten as passive material
- CSDA proton range in tungsten (Z=74)
- Tungsten density: 19.25 g/cm³
- Geometrical factor: 5x5 matrix of 4 mm² area sensor; about 1.5 kg detector (minimum) depending on the material in the region of contacts of the sensors

Energia	CSDA range	Range	Massa
300 MeV	99.33 g/cm ²	5.16 cm	2.5x2.5 → 620 g 2.0x2.0 → 397 g 1.5x1.5 → 223 g
350 MeV	127.1 g/cm ²	6.60 cm	2.5x2.5 → 795 g 2.0x2.0 → 508 g 1.5x1.5 → 286 g
400 MeV	156.8 g/cm ²	8.15 cm	2.5x2.5 → 979 g 2.0x2.0 → 627 g 1.5x1.5 → 353 g



HASPIDE-SPACE preliminary simulations with Fluka

75% of protons fully contained @ 400 MeV



- $4 \times 4 \text{ mm}^2$ of silicon $10 \text{ }\mu\text{m}$ thickness
- two kapton layers, $75 \text{ }\mu\text{m}$ thickness

	400 MeV		600 MeV	
Region	Mean (keV)	RMS (keV)	Mean (keV)	RMS (keV)
160	11.7	26.4	4.2	26.1
172	16.1	36.1	2.1	5.0

- Array 5×5 silicon detectors between two kapton foils on 5 layers, the front plane area is 4.8 cm^2

3.6-4 eV are needed to generate an electron-hole pair
Charge collection efficiency: 30-80%

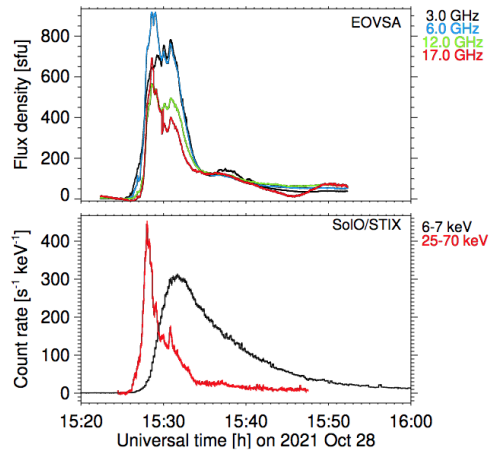


1906
UNIVERSITÀ
DEGLI STUDI
DI URBINO
CARLO BO

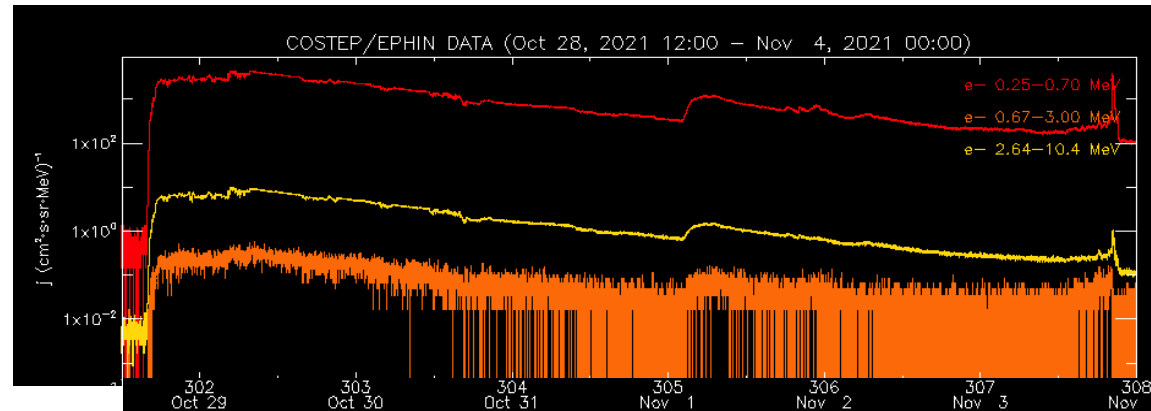


Monitoring the October 28, 2021 event with HASPIDE-SPACE: a case study

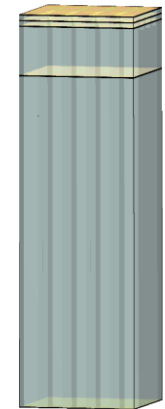
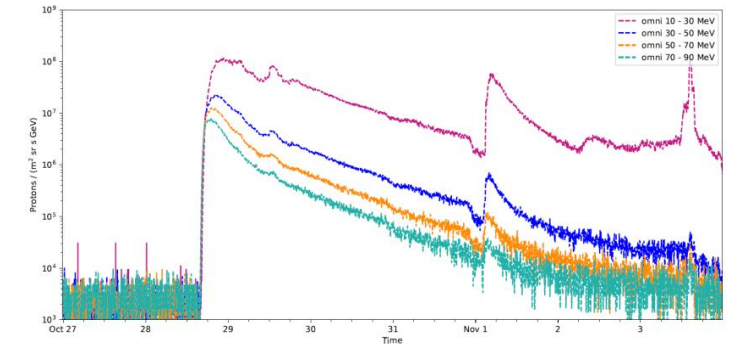
Onset 15:25 UT



Onset 16:00 UT



Onset 16.10 UT



1506
UNIVERSITÀ
DEGLI STUDI
DI URBINO
CARLO BO



a-Si:H detector present sensitivity: improvements are expected

→ photons: by considering the 3-40 keV energy interval the minimum detectable flux lies well below expected solar and nearby magnetar flux.

→ electrons: by considering electrons with energies > 50 keV: we are working in optimizing the first layers of sensors to lower the energy detection threshold.

→ protons: using the whole spectrum we obtain thousands of protons per second as minimum detectable signal (performance improves with stopping particles).

M. Menichelli et al., arXiv:2211.17114 submitted to Instruments

C. Grimani et al., arXiv: 2302.00339, submitted to Astroph. Sp. Sc.

Detection limits at 5σ for monochromatic photon fluxes.

Photon Energy [keV]	Minimum detectable flux [$\gamma/(\text{cm}^2 \text{ sr s})$]
3.0	$2.4 \cdot 10^3$
5.0	$3.8 \cdot 10^3$
10.0	$10.2 \cdot 10^3$
15.0	$20.2 \cdot 10^3$
20.0	$33.0 \cdot 10^3$
25.0	$47.8 \cdot 10^3$
30.0	$79.8 \cdot 10^3$
35.0	$150.0 \cdot 10^3$
40.0	$237.0 \cdot 10^3$

Detection limits at 5σ for monochromatic proton fluxes.

Proton Energy [MeV]	S/N = 5 Flux [$p (\text{cm}^2 \text{ sr s})^{-1}$]
5.0	$0.4 \cdot 10^3$
10.0	$0.5 \cdot 10^3$
20.0	$1.0 \cdot 10^3$
50.0	$1.5 \cdot 10^3$
70.0	$3.0 \cdot 10^3$
100.0	$3.5 \cdot 10^3$
200.0	$5.0 \cdot 10^3$
400.0	$10.0 \cdot 10^3$

Conclusions

- We are optimizing the design of an instrument to monitor solar activity, GRB, magnetar flaring for space weather applications
- Radiation hard hydrogenated amorphous silicon is considered as the active material
- Soft X-ray detection appears feasible. Working on hard X-ray detection
- Electron detection appears difficult, but improvements are possible
- The detection of protons during the peak of medium-to-strong events is feasible
- The instrument performance improves with the event intensity